

## Full Length Article

# Intrinsic material property differences in bone tissue from patients suffering low-trauma osteoporotic fractures, compared to matched non-fracturing women



S. Vennin<sup>b</sup>, A. Desyatova<sup>b</sup>, J.A. Turner<sup>b</sup>, P.A. Watson<sup>a</sup>, J.M. Lappe<sup>a</sup>, R.R. Recker<sup>a</sup>, M.P. Akhter<sup>a,\*</sup>

<sup>a</sup> Osteoporosis Research Center, Creighton University, Omaha, NE, United States

<sup>b</sup> University of Nebraska-Lincoln, NE, United States

## ARTICLE INFO

## Article history:

Received 11 August 2016

Revised 10 January 2017

Accepted 24 January 2017

Available online 27 January 2017

## Keywords:

Bone quality

Osteoporotic fractures

Nano-indentation testing

Intrinsic material properties

Fracture toughness

## ABSTRACT

Osteoporotic (low-trauma) fractures are a significant public health problem. Over 50% of women over 50 yrs. of age will suffer an osteoporotic fracture in their remaining lifetimes. While current therapies reduce skeletal fracture risk by maintaining or increasing bone density, additional information is needed that includes the intrinsic material strength properties of bone tissue to help develop better treatments, since measurements of bone density account for no more than ~50% of fracture risk. The hypothesis tested here is that postmenopausal women who have sustained osteoporotic fractures have reduced bone quality, as indicated with measures of intrinsic material properties compared to those who have not fractured. Transiliac biopsies (N = 120) were collected from fracturing (N = 60, Cases) and non-fracturing postmenopausal women (N = 60, age- and BMD-matched Controls) to measure intrinsic material properties using the nano-indentation technique. Each biopsy specimen was embedded in epoxy resin and then ground, polished and used for the nano-indentation testing. After calibration, multiple indentations were made using quasi-static (hardness, modulus) and dynamic (storage and loss moduli) testing protocols. Multiple indentations allowed the median and variance to be computed for each type of measurement for each specimen. Cases were found to have significantly lower median values for cortical hardness and indentation modulus. In addition, cases showed significantly less within-specimen variability in cortical modulus, cortical hardness, cortical storage modulus and trabecular hardness, and more within-specimen variability in trabecular loss modulus. Multivariate modeling indicated the presence of significant independent mechanical effects of cortical loss modulus, along with variability of cortical storage modulus, cortical loss modulus, and trabecular hardness. These results suggest mechanical heterogeneity of bone tissue may contribute to fracture resistance. Although the magnitudes of differences in the intrinsic properties were not overwhelming, this is the first comprehensive study to investigate, and compare the intrinsic properties of bone tissue in fracturing and non-fracturing postmenopausal women.

© 2017 Elsevier Inc. All rights reserved.

## 1. Introduction:

Osteoporosis is a significant public health problem, causing substantial clinical morbidity and health care expense. About 54 million Americans have osteoporosis or low bone mass, placing them at increased risk for low trauma fracture. When dual energy X-ray absorptiometry (DXA) became widely available to measure bone density in ~1990, the medical community adopted the idea that “osteoporosis” was a disease of low bone density/mass. However, since then it has become apparent that bone density measurements account for only about 50% of the variation in risk of fracture [1,2]. Indeed, most of the low-trauma fractures

occurring after age 50 in the U.S. occur in patients with bone DXA values that are above the T-score that the World Health Organization (WHO) defines as osteoporosis (i.e. <−2.5) [3,4]. Thus at least one half of the risk of low-trauma fracture remains unexplained. Our contribution here is to provide a better understanding of intrinsic bone tissue material properties affecting bone quality that may be important contributors to risk of low trauma fractures. This contribution is a step in the continuum of research that we hope will lead to development of therapeutic strategies that will further reduce the incidence of osteoporotic fractures.

Excessive remodeling can make the bone tissue more fragile as bone formation/mineralization lags behind resorption at newly formed remodeling sites, thus rendering bone tissue weak and compliant due to poor intrinsic material strength properties [5,6]. On the other hand, suppression of bone remodeling may cause the bone tissue to be more

\* Corresponding author at: ORC, Creighton University, Suite 4820, 601 North 30th Street, Omaha, NE, United States.

E-mail address: [akhtermp@creighton.edu](mailto:akhtermp@creighton.edu) (M.P. Akhter).

mineralized thus increasing its brittleness and resulting in a greater accumulation of microdamage [7–11]. The increased microdamage may affect the intrinsic material properties of bone tissue making it more susceptible to fractures. In addition, age-related risk of skeletal fracture is well documented [3,4,12,13]. This increased fracture risk is only partially explained by reduced bone mass or density, suggesting that other factors may be responsible for the age-related increase in fracture risk such as intrinsic material properties of bone tissue.

For more than two decades, bone mass and density have been measured accurately and easily by radiologic techniques, and the correlation between the amount of bone and its ability to withstand loads is significant [14]. However, recent experience has led to the realization that bone mass and density, by any of the measures we commonly use, are not the only factors affecting the skeleton's ability to resist failure, i.e., fracture. Thus we propose that, in addition to bone mass and density, the intrinsic material properties of bone tissue, along with its geometric arrangement, are very critical in defining bone quality.

Our primary hypothesis is that the postmenopausal women with osteopenia who have sustained low-trauma fractures have changes in measures of intrinsic mechanical properties including quasi-static hardness, indentation modulus, along with dynamic storage and loss moduli, compared with those with the same degree of osteopenia who have not fractured.

## 2. Materials and methods

### 2.1. Participants

As part of an NIH-funded (1 R01 AR054496-01A1) project, 120 postmenopausal women were recruited for a study of bone quality. The fracture group (cases) included 60 post-menopausal women with osteopenic BMD values (T-scores between  $-1.0$  and  $-2.5$  for either the hip or spine), who were between ages 45 and 80, had a fracture during the previous 5 years from low trauma, but were otherwise healthy (Table 1). “Low trauma” was defined as any fracture caused by trauma equal to, or less than, a fall to the floor from a standing height, excluding fractures of the digits, face or skull. These would be considered classical osteoporotic fractures. Details of the fracture types for the Cases are in Table 1. At least one vertebral fracture was reported in 23 individuals. In contrast, six of the Controls had a history of fracture, none were low trauma, all were from motor vehicle accidents, or similar levels of trauma. None of the women in either group were on any anti-resorptive (bisphosphonate, calcitonin, estrogen, etc.) or bone forming (PTH) agents and the control group consisted of 60 post-menopausal women who had no prevalent osteoporotic fractures (by history or spine x-ray) on entry into the study. As in the fracturing group, all of the control

subjects were between ages 45 and 80, had T-scores between  $-1.0$  and  $-2.5$  for either the hip or spine, and were otherwise healthy. Each fracturing subject was matched with a control subject who was similar in age and within 10% of BMD. The matching was performed immediately after the successful enrollment of each fracturing subject.

Two transiliac biopsy specimens were obtained from each of the 120 subjects, fracturing (N = 60, cases) and non-fracturing postmenopausal women (N = 60, matched normal controls) to measure intrinsic material properties using the nano-indentation technique. Biopsies were performed using well-established techniques [15–17]. One specimen for each participant was embedded and tested with nanoindentation, the other was used for histomorphometry, to be reported in a separate publication. To prepare the sample for indentation, each bone biopsy was carefully cleaned of bone marrow using a soft jet of ionic water [18]. After removing the residual water via centrifuge at 3000 rpm for 30 s [19] while retaining the water located in the bone tissue (the tissue remained in the hydrated state during storage and testing), the biopsy was embedded in low viscosity EpoThin (Buehler, IL) embedding material. EpoThin epoxy uses resin and hardener (1:3 ratio) similar to previous studies [20,21]. The embedding material flows into the small crevices, cracks, holes, etc., and hardens within 24 h without penetrating or diffusing into bone tissue itself. The Epo Thin embedding material provides mechanical support to the bone tissue being tested under the compressive force of nano-indentation [20,22–25]. Each biopsy was processed similarly ensuring that the procedure remained consistent over time. The embedded specimens were subjected to grinding using a motorized polishing wheel (Ecomet-3, and Automet-2, Buehler, IL) with interchangeable silicon carbide discs of diminishing grit size (320, 600, 800, 1200  $\mu\text{m}$ ) under irrigation with deionized water. Finally, each specimen was metallographically polished to produce the smooth surfaces using a series (1, 0.5, 0.05  $\mu\text{m}$ ) of alumina powder slurries on neoprene polishing cloth (Buehler) and rinsing with ionic water in between slurries [20,26,27]. The other specimen was embedded in polymethylmethacrylate and used for all the other studies, i.e., micro-CT, Histomorphometry, FTIR (Fourier transform infrared) spectroscopy, [28] Raman, and high resolution microscopy (data are not reported here).

**Nanoindentation:** Previous nanoindentation studies, measuring both elastic and plastic properties in bone tissue, have been reported [20,26, 27,29–32]. Nanoindentation is a method for estimating the intrinsic compressive mechanical properties (i.e. stiffness and pre-failure, post-yield properties) of bone. Fig. 1 is a schematic of the nanoindentation showing the components of the procedure. First, a series of indentations (TI 950 TriboIndenter, Hysitron, MN) in the polished surface of a standard fused quartz material are used to calibrate the tip area function for the diamond Berkovich tip used here (tip radius 150 nm, Fig. 1).

**Table 1**  
Subject characteristics.

	Cases (N = 60)	Control (N = 60)	SSD
Age (years $\pm$ SD)	62.5 $\pm$ 7.4	62.2 $\pm$ 7.3	$-0.0017 \pm 0.0948$
BMD [ $\text{g}/\text{cm}^2$ ] of the hip, mean (SD)	0.826 $\pm$ 0.087	0.827 $\pm$ 0.082	0.2529 $\pm$ 2.8186
Years since menopause (SD)	16.7 $\pm$ 9.5	15.5 $\pm$ 10.8	0.9956 $\pm$ 11.1766
BMD of the hip T-score, mean (SD)	$-0.952 \pm 0.713$	$-0.953 \pm 0.657$	0.0013 $\pm$ 0.7603
Low trauma fractures (n)		<sup>b</sup>	
Wrist	20	0	
Ankle	16	0	
Humerus	7	0	
Patella	4	0	
Shoulder	3	0	
Elbow	2	0	
Hip	2	0	
others (fibula, foot, knee, lower leg, pelvis, and wrist & elbow combined)	6	0	
Vertebral <sup>a</sup>	23	0	

SSD—Mean difference and SD of difference.

<sup>a</sup> At least one vertebral fracture was reported in 23 individuals.

<sup>b</sup> Six of the Controls had a history of fracture, none were low trauma, all were from motor vehicle accidents, or similar levels of trauma.

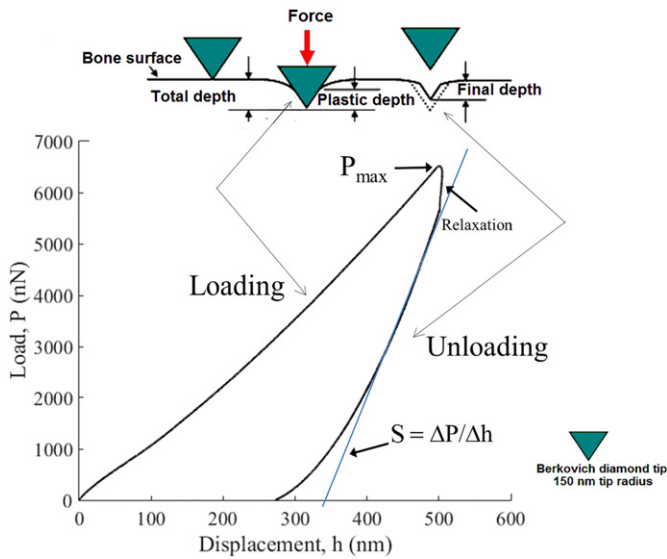


**Fig. 1.** Nano-indentation (quasi-static) testing schematics showing diamond tip during loading and unloading part of the nano indentation testing [102]. Plastic (solid line) and elastic (dashed line) part of the indent is shown on bone surface. Maximum height of the load-displacement diagram represents force or load ( $P_{\max}$ ) used to calculate hardness ( $H$ ). The slope of the unloading part of the curve represents stiffness ( $S$ ). The unloading portion of the curve, after the relaxation, was used to determine properties for all samples.

Then, for each bone specimen multiple indentations were made using two techniques as explained below:

## 2.2. Quasi-static nanoindentation testing

Using the quasi-static testing mode [20,26,27,29–32], several indents ( $N = 25$  indents per bone type, total 50 indents/biopsy, each indent separated by  $10 \mu\text{m}$ ) were made on both cortical and trabecular bone (Fig. 2) using a target depth of  $500 \text{ nm}$  at a constant loading rate of  $50 \text{ nm/s}$  including a preliminary thermal drift rate correction limited to a maximum of  $0.05 \text{ nm/s}$ . Using scanning probe microscopy (SPM) with the indenter tip, the average measured surface roughness was  $\sim 50 \text{ nm}$  [26]. The indentation depth,  $500 \text{ nm}$ , is such that minor surface roughness does not play a role in the measurements as the contact depth is 10 times the average roughness [26,33] (Polly, et al. 2012; Donnelly et al. 2006). Regions of interest on the biopsy were first identified using SPM imaging to quantify the surface topography. After

imaging, the indent positions were chosen randomly within the regions deemed to have an appropriate level of roughness [26]. In cortical bone, indent sites were in interstitial bone and not within osteons. Interstitial bone is at a relatively steady state status (less mineral variation) due to its age with regards to “mineral/matrix” composite, and thus more prone to microdamage [27,34–39]. The indents on the cortical bone were placed along a line parallel to the periosteal surface as shown in Fig. 2A. The indents on the trabecular bone were in the center of each trabecula avoiding edges (Fig. 2A) [26,40–42]. Selections of all the indent sites were done by identifying the region of interests using SPM imaging without knowing the specimen group/code. For the displacement-controlled quasi-static nanoindentation testing used here [43], the indenter tip is pushed into the specimen to a prescribed depth ( $500 \text{ nm}$ ), while the load on the indenter tip was measured. The indentation procedure includes a linear loading period of  $10 \text{ s}$ , a holding period at a maximum load of  $10 \text{ s}$  and a linear unloading period of  $10 \text{ s}$ . Prior to unloading, the  $10 \text{ s}$  constant-depth hold period minimizes the viscoelastic (time dependent) deformation. To minimize time-dependent effects the 50% to 95% region of each unloading curve is used for calculation of elastic properties. The load-displacement data from each indentation are used to calculate the indentation modulus ( $E_i$ ) from the slope of the load displacement curve, and hardness ( $H$ ) from the maximum height of the load displacement curve. The well-documented Oliver-Pharr method [29] was used to extract the indentation modulus (relation-1) and hardness (relation-2) from the force-displacement curves. The indentation modulus ( $E_i$ ) was calculated from the unloading portion of the force-displacement curve according to the relation [29]:

$$E_i = \left[ \frac{2}{S} * \sqrt{\frac{A_c}{\pi}} - (1 - \nu_t^2) / E_t \right]^{-1} = E_s / (1 - \nu_s^2) \quad (1)$$

and the hardness from the relation:

$$H = P_{\max} / A_c \quad (2)$$

where  $E$  ( $E_s$ ,  $E_t$ , for bone sample and indenter tip material) and  $\nu$  ( $\nu_s$ ,  $\nu_t$ , for bone sample and indenter tip) are elastic moduli and Poisson's ratios respectively. The Poisson's ratio of  $0.3$  [18,44,45–47] was used for bone tissue.  $S$  and  $P_{\max}$  are contact stiffness and maximum load on the load-displacement curve. In addition,  $A_c$  is the contact area of the indenter tip-sample contact during the maximum load. The bone tissue hardness [cortical - Cort-H, Trabecular - Trab-H], indentation modulus [cortical - Cort-E, Trabecular - Trab-E] and sample variance (variances of the 25 observations) [cortical -  $S_v$ -Cort-H, Trabecular -  $S_v$ -Trab-H] are reported for quasi static testing (Table 2).

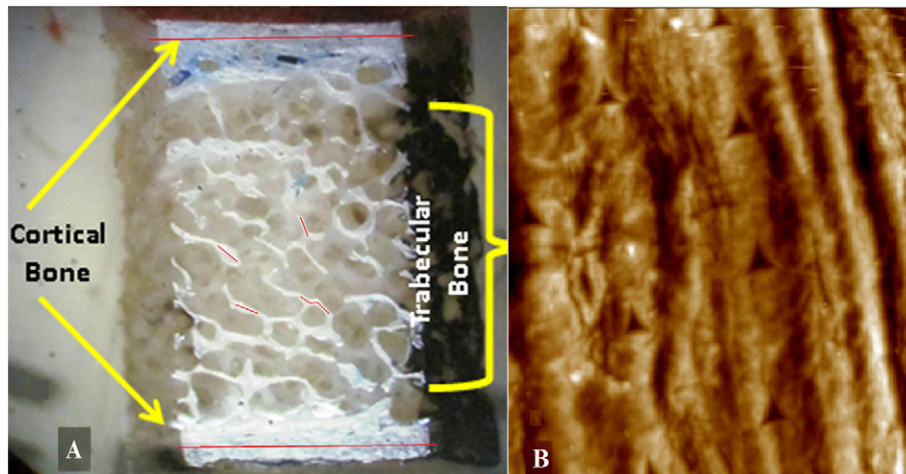


**Fig. 2.** Regions of indent sites include both cortical and trabecular bone (A) in transiliac bone biopsy specimens prepared for nanoindentation testing. Red lines show placements of indents (parallel to the periosteal surface in cortical bone and in the center of selected trabeculae). Examples of indents are shown (dark triangles) in a  $50 \mu\text{m} \times 50 \mu\text{m}$  trabecular region (B).

**Table 2**  
Nano-indentation data. Cases vs. controls.

Variable	Cases (N = 60) Median (IQ <sup>c</sup> range)	Control (N = 60) Median (IQ range)	<sup>a</sup> s	p(s)	<sup>b</sup> %
<b>Quasi-static testing</b>					
<b>Cortical</b>					
Modulus-(GPa) Cort-E	13.47 (9.96–16.71)	14.88 (12.43–18.42)	– 279.0	0.039	9.44
Variance S <sub>V</sub> -Cort-E	2.19 (1.02–5.02)	4.43 (1.95–7.18)	– 410.0	0.002	50.57
Hardness-(GPa) Cort-H	0.43 (0.31–0.52)	0.49 (0.29–0.66)	– 271.0	0.045	12.24
Variance S <sub>V</sub> -Cort-H	0.0072 (0.0036–0.0144)	0.0110 (0.0049–0.0196)	– 286.0	0.034	34.39
<b>Trabecular</b>					
Modulus (GPa) Trab-E	14.13 (11.36–16.48)	14.18 (12.37–16.34)	– 61.0	ns	0.39
Variance S <sub>V</sub> -Trab-E	2.76 (1.50–4.31)	3.46 (2.08–6.03)	– 221.0	ns	20.30
Hardness- (GPa) Trab-H	0.41 (0.32–0.47)	0.41 (0.34–0.46)	– 110.5	ns	0.00
Variance S <sub>V</sub> -Trab-H	0.0049 (0.0025–0.0064)	0.0064 (0.0036–0.01)	– 275.5	0.042	23.44
<b>Dynamic testing<sup>d</sup></b>					
<b>Cortical</b>					
Storage Modulus (GPa) Cort-E'	15.14 (12.62–19.02)	16.04 (13.56–18.70)	– 1.3	ns	5.64
Variance S <sub>V</sub> -Cort-E'	2.42 (1.37–4.39)	3.76 (2.40–6.13)	– 391.0	0.003	35.75
Loss Modulus (GPa) Cort-E''	0.57 (0.38–0.88)	0.64 (0.47–0.81)	7.0	ns	10.85
Variance S <sub>V</sub> -Cort-E''	0.026 (0.013–0.070)	0.017 (0.0087–0.048)	249.0	ns	– 51.48
Cort-Tan-δ (E''/E')	0.038 (0.027–0.05)	0.04 (0.029–0.049)	82.0	ns	3.75
<b>Trabecular</b>					
Storage Modulus (GPa) Trab-E'	16.11 (14.55–19.35)	16.69 (15.40–18.77)	– 29.0	ns	3.48
Variance S <sub>V</sub> -Trab-E'	2.51 (1.72–4.04)	2.77 (1.88–4.45)	– 69.0	ns	9.38
Loss Modulus (GPa) Trab-E''	0.54 (0.36–0.65)	0.56 (0.43–0.68)	54.0	ns	3.57
Variance S <sub>V</sub> -Trab-E''	0.024 (0.011–0.053)	0.012 (0.005–0.040)	380.5	0.004	– 98.76
Trab-Tan-δ (E''/E')	0.031 (0.021–0.042)	0.036 (0.022–0.04)	44.0	ns	12.50

<sup>a</sup> s-Nonparametric Wilcoxon signed rank test; p(s)- p value from the Wilcoxon test for the Cases vs. Control

<sup>b</sup> %-Case-control median difference as percent of control (note that medians provided in the table are rounded while percent differences were calculated with unrounded medians)

<sup>c</sup> IQ-interquartile range (25th percentile – 75th percentile)

<sup>d</sup> Please note that the values for E', E'', and Tan-δ represent at the mid-range dynamic frequency of 105 Hz.

### 2.3. Dynamic nanoindentation testing

To determine the intrinsic viscoelastic material properties, dynamic nanoindentation testing was used [26]. Similar to quasi-static testing, the indenter tip was loaded at a rate of 50 μN/s and then held at the maximum load of 6 mN comparable to the maximum load in the quasi-static measurements. However, for dynamic tests, a small sinusoidal force was superimposed onto the quasi-static force during the holding section, causing the tip to oscillate about its equilibrium indentation depth with small displacement amplitude. Dynamic force amplitudes in the range of 75–125 μN caused displacement amplitudes of few nanometers. During the holding period, the dynamic load frequency was adjusted incrementally between 10 and 200 Hz using 32 equally spaced steps. At each frequency a lock-in amplifier measured the displacement amplitude and phase lag of the displacement response relative to the input forcing signal. The dynamic testing provides the storage modulus [E'], representing the ability of the material to store recoverable energy, and the loss modulus, [E''], representing the deformation that is not recoverable. We performed dynamic testing similar to what is described by Donnelly et al. [48] and Polly et al. [26]. Compared to published data, [48] we observed a similar trend in our data (in loss modulus, storage modulus, and loss tangent data) for the dynamic frequency range of 10 Hz to 200 Hz [26]. However, for comparison purposes, the data are reported at the mid-range frequency of 105 Hz. The bone tissue storage modulus [cortical-Cort-E', Trabecular-Trab-E'], loss modulus [cortical-Cort-E'', Trabecular-Trab-E''], and sample variance (material heterogeneity) (cortical - S<sub>V</sub>-Cort-E' & E'', Trabecular-S<sub>V</sub>-Trab-E' & E'') are reported for dynamic testing (Table 2). The loss tangent (or damping) is a dimensionless expression defined by TanDel [tan δ] = (E'')/(E') that defines the range of behavior from purely elastic (tan δ = 0) to purely viscous (tan δ = 1).

For each type of bone tissue (trabecular and cortical), 25 indents were analyzed within a biopsy. Thus a total of 50 indents were performed on each biopsy for each type (quasi-static and dynamic-N =

100 tests/biopsy) of nanoindentation testing. Indents were kept at least 10 μm distance apart from each other (Fig. 2). Means and variances of the 25 observations of each type of bone tissue were calculated for each biopsy, and these were used as measures of the overall level of the variable and the within-specimen heterogeneity (amount of variation), respectively, of the variable for each subject.

### 2.4. Statistics

The analyses of these data included descriptive statistics. Cases and controls were compared using the Wilcoxon signed rank test to compare the medians and the heterogeneity of each nanoindentation parameter. In addition, modeling using conditional multivariate logistic regression was used to evaluate the efficacy of combinations of nanoindentation variables in accounting for fracture risk. All variables were standardized for use in multivariate logistic regression. A full model including all the nanoindentation variables was evaluated, then backwards elimination was used to produce a reduced model including only the variables with significant (p < 0.05) explanatory power. In addition, using Pearson correlation coefficients, the relationship between nanoindentation variables and the published mineral composition properties (Fourier transform infrared FTIR spectroscopy) [28], were determined. The FTIR spectroscopy [28] was performed in a set of separate bone biopsies from the same cohort of women. Finally, nanoindentation measures were compared between cortical and trabecular bone along with quasi-static (E) and dynamic (E') in pooled subjects (fracture cases and controls) using the Wilcoxon signed rank test. Only comparisons between the E and E' were performed as they are compatible measurements reflecting resistance to indents.

### 3. Results

The 60 cases had a mean (± standard deviation) age at biopsy of 62.5 (7.4) compared to control mean age of 62.2 (7.3) year. Ages for both



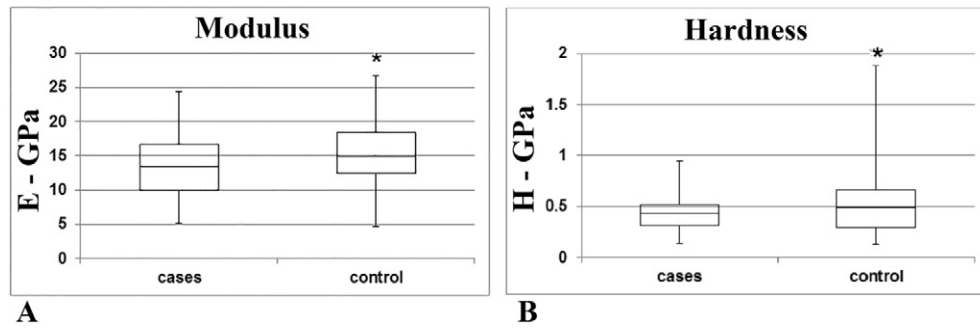


**Fig. 3.** Box-and-whisker plots for A) elastic modulus, B) hardness in cortical bone. \* Difference between cases and controls ( $p < 0.05$ ). Bottom and the top of the box plot represent the lower (25%) and the top (75%) quartiles, respectively. The upper and the lower bounds of the error bars represent the range of the data.

cases and controls ranged from 48 to 80 years. Cases had a mean hip BMD of 0.826 (0.087) g/cm<sup>2</sup> compared to control mean hip BMD of 0.827 (0.082) g/cm<sup>2</sup>. Hip BMD ranged from 0.647 to 1.113 g/cm<sup>2</sup> (Table 1).

There were significant differences between Cases and Controls in several of the intrinsic material property variables and in their sample variance (heterogeneity), for both quasi-static and dynamic testing as measured by nanoindentation. The descriptive statistics and p-values (Wilcoxon signed rank test, nonparametric) for the entire data set are included in Table 2.

### 3.1. Cortical bone

Median values for both cortical indentation modulus and hardness were significantly greater in the Control group as compared to the Cases (Table 2, Fig. 3). Importantly, tissue mechanical heterogeneity in all the measured variables except loss modulus, as expressed by the term variance ( $S_v$ ), was significantly greater in the control group. For instance, the values for variance in cortical modulus, and hardness (*quasi static testing*) are significantly higher in the Controls as compared to the Cases. In addition, the dynamic testing showed significant difference in the value for variance of storage modulus only (Table 2). The variance in cortical storage modulus was 35.75% higher in Controls as compared to the Cases. On the other hand, variance in the loss modulus was 51.48%

higher in the Cases compared to the Controls, a difference which fell just short of statistical significance ( $p < 0.07$ ).

### 3.2. Trabecular bone

Although differences in trabecular hardness and modulus (*for both quasi-static and dynamic testing*) were not significant between Control and Cases, the sample variance in hardness and loss modulus were different. Variance in trabecular hardness was 23.44% higher in the Controls as compared to the Cases. While variance for the storage modulus ( $S_v$ -Trab-E') was not different, the value for variance in the trabecular loss modulus was significantly greater (98.76%) in Cases as compared to the Controls (Table 2).

Multivariate logistic regression: The results of this analysis are shown in Table 3. The full model reached  $R^2 = 0.432$ . The reduced model had  $R^2 = 0.355$ , and included 4 variables: within-specimen variability in cortical storage modulus, within-specimen variability in cortical loss modulus, and within-specimen variability in trabecular hardness, along with median cortical loss modulus. Except in the case of within-specimen variability of cortical loss modulus, all variables were negatively associated with fracture risk (higher levels in the control group).

Additional logistic regression models were evaluated, adding age, hip BMD, age by BMD interaction, interactions of the nanoindentation

**Table 3**

Conditional Maximum Likelihood Estimates from multivariate logistic regression of Case vs Control.

Variable	DF	Estimate	Standard error	Wald chi-square	Pr > ChiSq	Odds ratio point estimate	95% confidence limits	
Full model								
Cort-E	1	−0.923	0.784	1.386	0.2391	0.397	0.085	1.848
S <sub>V</sub> -Cort-E	1	−0.238	0.491	0.235	0.6275	0.788	0.301	2.064
Cort-H	1	−0.079	0.673	0.014	0.9068	0.924	0.247	3.456
S <sub>V</sub> -Cort-H	1	0.409	0.612	0.446	0.5042	1.505	0.453	4.997
Cort-E'	1	0.702	0.812	0.748	0.3873	2.018	0.411	9.916
S <sub>V</sub> -Cort-E'	1	−0.956	0.440	4.708	0.03	0.385	0.162	0.912
Cort-E''	1	−0.859	1.038	0.686	0.4077	0.423	0.055	3.237
S <sub>V</sub> -Cort-E''	1	1.299	0.733	3.140	0.0764	3.667	0.871	15.430
Cort- Tan-δ	1	1.173	3.385	0.120	0.729	3.231	0.004	>999
Trab-E	1	0.312	0.528	0.350	0.5539	1.367	0.486	3.846
S <sub>V</sub> -Trab-E	1	0.142	0.443	0.103	0.7488	1.152	0.484	2.744
Trab-H	1	0.249	0.385	0.419	0.5174	1.283	0.603	2.727
S <sub>V</sub> -Trab-H	1	−1.110	0.508	4.781	0.0288	0.329	0.122	0.891
Trab-E'	1	−0.293	0.806	0.132	0.7164	0.746	0.154	3.621
S <sub>V</sub> -Trab-E'	1	−0.128	0.332	0.148	0.7002	0.880	0.459	1.687
Trab-E''	1	−0.889	2.059	0.187	0.6658	0.411	0.007	23.247
S <sub>V</sub> -Trab-E''	1	0.265	0.459	0.334	0.5633	1.303	0.531	3.201
Trab- Tan-δ	1	0.726	2.071	0.123	0.7259	2.067	0.036	119.736
Reduced model								
S <sub>V</sub> -Cort-E'	1	−0.895	0.317	7.984	0.0047	0.408	0.220	0.760
Cort-E''	1	−0.649	0.308	4.437	0.0352	0.522	0.285	0.956
S <sub>V</sub> -Cort-E''	1	1.270	0.488	6.783	0.0092	3.560	1.369	9.257
S <sub>V</sub> -Trab-H	1	−0.660	0.315	4.404	0.0358	0.517	0.279	0.957

$S_v$ - sample variance; Cort-cortical bone; Trab-trabecular bone; E-modulus(GPa); H-hardness(GPa); E'-storage modulus(GPa); E''-loss modulus (GPa).

**Table 4**  
Correlations (Pearson Correlation Coefficients) of bone tissue's mineral and matrix (FTIR) [28] with intrinsic material properties (nanoindentation).

	E	H	E'	E''
Cortical				
Mineral/matrix	0.112	0.131	0.113	0.035
Carbonate/phosphate	0.043	0.131	0.02	0.097
Trabecular				
Mineral/matrix	0.146	0.134	0.087	0.137
Carbonate/phosphate	0.065	0.172	0.016	0.045

E-modulus (GPa); H-hardness (GPa); E'-storage modulus (GPa); E''-loss modulus (GPa). All the correlations are non-significant.

variables with age and hip BMD, and interactions among the nanoindentation variables. No additional significant effects were observed in these analyses (results not shown).

A comparison between the nanomechanical property and published compositional data (Boskey et al., 2015, JBMR) [28] from the same cohort of women but from separate biopsies processed differently (e.g. hydrated bone tissue in epoxy resin for nanomechanical vs. dehydrated tissue embedded in PMMA for FTIR technique)) showed no significant relationship between mineral/matrix and nanoindentation variables, nor between carbonate/phosphate (C/P) and nanoindentation variables (Table 4).

Finally, significant differences between cortical and trabecular bone were observed in several measures. While hardness, loss modulus, and Tan delta ( $\delta$ ) were higher in cortical bone, storage modulus was higher in trabecular bone (Table 5, "a"). However, quasi-static modulus (E) shows no differences between cortical and trabecular bone.

In addition, dynamic storage (E') modulus was greater (Table 5, "b") than quasi-static (E) modulus in the pooled subjects for both cortical and trabecular bone tissue. Furthermore, using Fisher's test of Spearman correlation coefficients, we found a significant correlation between

**Table 5**  
Nano-indentation data. Trabecular vs. cortical and quasi-static vs. dynamic measurements.

Variable	Pooled (cases and controls) Median (IQ range)
Quasi-static testing	
Cortical	
Modulus-(GPa) Cort-E	14.18(10.92–17.63) <sup>b</sup>
Variance $S_V$ -Cort-E	2.976(1.381–5.882)
Hardness-(GPa) Cort-H	0.47(0.305–0.63) <sup>a</sup>
Variance $S_V$ -Cort-H	0.008(0.004–0.017) <sup>a</sup>
Trabecular	
Modulus (GPa) Trab-E	14.16(12.01–16.35) <sup>b</sup>
Variance $S_V$ -Trab-E	3.10(1.76–5.22)
Hardness- (GPa) Trab-H	0.41(0.33–0.465) <sup>a</sup>
Variance $S_V$ -Trab-H	0.005(0.003–0.008) <sup>a</sup>
Dynamic testing <sup>c</sup>	
Cortical	
Storage Modulus (GPa) Cort-E'	15.93(13.04–18.8) <sup>a,b</sup>
Variance $S_V$ -Cort-E'	2.94(1.74–5.93)
Loss Modulus (GPa) Cort-E''	0.615(0.41–0.835) <sup>a</sup>
Variance $S_V$ -Cort-E''	0.023(0.01–0.058) <sup>a</sup>
Cort-Tan- $\delta$ (E''/E')	0.039(0.028–0.05) <sup>a</sup>
Trabecular	
Storage Modulus (GPa) Trab-E'	16.475(14.79–19.075) <sup>a,b</sup>
Variance $S_V$ -Trab-E'	2.657(1.769–4.203)
Loss Modulus (GPa) Trab-E''	0.55(0.39–0.675) <sup>a</sup>
Variance $S_V$ -Trab-E''	0.017(0.006–0.048) <sup>a</sup>
Trab-Tan- $\delta$ (E''/E')	0.034(0.022–0.041) <sup>a</sup>

<sup>a</sup> p (< 0.05) cortical vs trabecular difference-Wilcoxon test; pooled fracture cases and controls

<sup>b</sup> p (< 0.05) quasi-static modulus (E) vs dynamic storage modulus (E') difference-Wilcoxon test.

<sup>c</sup> Please note that the values for E', E'', and Tan- $\delta$  represent at the mid-range dynamic frequency of 105 Hz.

modulus (E) and storage modulus (E') for both cortical [ $r = 0.68$ ] and trabecular [ $r = 0.75$ ] bone tissue.

#### 4. Discussion

The overall goal of this project was to find a bone quality measure(s) that is independent of bone mass and helps to differentiate between fracturing (Cases) and non-fracturing (Controls) individuals. Significant differences were noted in the nanoindentation test variables, particularly variance (both quasi-static and dynamic) between the Controls and Cases. Higher values for variance are noted in the Controls for all but one variable, ( $S_V$ -Trab-E''). These differences may reflect the heterogeneity in the intrinsic properties of bone tissue (cortical and trabecular) that is different between Controls and Cases and thus helps explain the increased fracture risk in Cases. Heterogeneity or degree of heterogeneity as measured by variance or coefficient of variance (COV), in material properties is a standard approach and has been reported previously [33,49–54]. Heterogeneity in materials offers resistance or discontinuity in the propagation of microcracks and therefore, enhances its toughness property [32,37,49,55].

The cortical bone tissue in the Controls had both greater hardness and indentation modulus as compared to the Cases. In addition, higher values for variance in the quasi-static and dynamic material properties for both the cortical and trabecular bone (Table 2) in Controls indirectly suggest that the bone tissue is more heterogeneous and therefore tougher than Cases. Although fracture toughness was not measured directly [56–61], the greater heterogeneity (greater values for variance) in hardness and indentation modulus often indicates higher toughness, and could give rise to more fracture-resistant bone in the Control group.

Our data from both quasi-static and dynamic testing are similar to the data in most of the published studies. For instance, the trabecular median values in the non-fracturing post-menopausal controls, for indentation modulus (14.18 GPa), hardness (0.41 GPa), storage modulus (16.69 GPa), and loss modulus (0.56 GPa) are comparable with what has been reported in iliac crest biopsies from healthy post-menopausal women (both static and dynamic testing) [26], osteoporotic women [41], and in fracturing and non-fracturing controls (quasi-static testing only) [62]. However, there were also some differences compared with the published values [42] for modulus and hardness. Although the cancellous/trabecular bone tissue's indentation modulus was greater than reported here, Kim et al. [42] showed a significant decline in the osteoporotic as compared to non-osteoporotic vertebral body specimens. Any difference in nanoindentation data (modulus, hardness, etc.) could be due to specimen's source (vertebral body, iliac crest, femoral head, etc.) [42,63,64], its preparation, and testing techniques.

The mineral composition (FTIR) [28] and mechanical property data (Table 4) show no significant relationship between mineral/matrix and nanoindentation variables, nor between carbonate/phosphate (C/P) and nanoindentation variables. This may suggest other factors [65] responsible for the mechanical property differences between Cases and Controls that need further investigation. In most studies, the bone mechanical properties are shown to be sensitive to mineral composition when measured in proximity of each other [21,42,66–70]. The declining mineral: matrix ratio was reported to be responsible for lower indentation modulus and hardness in trabeculae of osteoporotic vertebral bodies [42]. However, others [65] showed no relationship between mineral composition and indentation modulus in fracturing cases and controls and suggested that stiffening of the collagen matrix could also be responsible for fractures.

Histomorphometric variables such as bone turnover [41] and bone formation rate [62,71] have inverse relationships with mechanical properties (hardness, modulus). These published data [41] also suggest that the mechanical properties in biopsies from fracturing patients and with severely suppressed bone turnover, were greater and had less variability in cortical indentation modulus than controls. Our data indicate

that fracture Cases have less variability and heterogeneity than non-fracture Controls [54,62,72–74].

The nanoindentation data are important to understand the role of local mechanical properties of bone tissue towards the whole bone strength. Some of the animal data from our lab [20,31] suggest that the local indentation material property of hardness and indentation modulus agree with whole bone strength properties. Although tested bone tissue is not the fracture site, we propose that local intrinsic material properties and their variation affect the whole bone properties at the organ level, and therefore, help in predicting skeletal fragility.

Several studies suggest that the spatial variation of material and mineral distribution properties (i.e. heterogeneity) affect bone toughness and energy dissipation through stress/strain distribution in bone tissue [49,62,75,76]. Each triangular shaped indent (1 to 5  $\mu\text{m}$  length for each side, Fig. 2B) represents an intrinsic material test of bone tissue which is locally uniform/homogeneous and anisotropic in structure [27, 30,77]. Each tested site (locally uniform) may differ in nanoscale level structural properties (mineralized collagen fibrils, size/shape of the mineral crystals) from other sites [32,50,51]. Thus, any variation in the nano level structural properties of bone tissue may influence the local intrinsic material strength properties. More variation in the local tissue properties may produce greater variation in the tissue strength properties and is a reflection of heterogeneity (variation) in bone tissue. The nano level heterogeneity (measured from COV) in bone tissue is good for toughness or energy absorption ability that is critical in fracture prevention (Yao et al. 2011) [32].

The nano level structure helps the energy absorption due to its deformation at the fibrils, and enhances the intrinsic toughness of bone tissue [49,51,54,78,79]. One possible explanation for heterogeneity-related advantages in materials was given by Tai et al. [49], suggesting that while homogenous materials deform locally and produce extensive damage, heterogeneous materials allow the damage to be diffused and carried by the surrounding tissue allowing for more energy absorption capability or toughness.

Dynamic mechanical testing provides quantification of the viscoelastic properties of bone tissue [48,80]. The median values for storage  $[E']$  and loss moduli  $[E'']$  between cases and controls were not different (both cortical and trabecular tissue). While the variance for cortical  $E'$  was smaller, it was greater for trabecular  $E''$  in Cases as compared to Controls. Additional work is recommended to understand if such a difference in loss modulus variance may reflect higher damage/energy dissipation ability in the Cases.

With regards to “storage/loss modulus”, we expected that more mineralized bone tissue would have a larger “storage modulus” (the stiffness component of the material response) and a lower loss modulus (the energy dissipation component of the material response). However, our results suggest that the relationship among storage, loss, modulus, mineral, etc. is much more complex. Lower loss tangent (loss modulus/storage modulus ratio  $[E''/E']$ ) will suggest a less compliant tissue [48]. For instance, Donnelly et al., 2006 [48] reported that the lamellar bone tissue in cancellous bone tissue (human vertebrae) was stiffer and harder than the interlamellar tissue and reflected lower compliance in terms of loss tangent ( $E''/E'$ ) or lower loss modulus ( $E''$ ).

The greater hardness in cortical as compared to trabecular bone tissue agrees with the published data from nanoindentation testing [46]. The lack of significant difference for quasi-static modulus between cortical and trabecular bone tissue was also reported in previous investigations [81–83]. These data suggest that, intrinsically, the quasi-static moduli for cortical and trabecular bone are similar. However, as compared to cortical bone, the greater storage ( $E'$ ) modulus (as reflected in Loss tangent or Tan delta  $[E''/E']$ ), in trabecular bone suggest that it is less compliant [48]. Despite greater hardness in the cortical bone tissue, its decreased storage modulus reflects a more compliant tissue - an observation not in agreement with the reported data [48].

Finally, with regards to dynamic ( $E'$ ) vs. quasi-static ( $E$ ), both cortical and trabecular bone show a greater storage modulus ( $E'$ ) as

compared to the modulus ( $E$ ) as observed previously [26] and are highly correlated ( $r = 0.68$  and  $0.75$ ). These data suggest that while  $E$  is purely an elastic and  $E'$  is a viscoelastic response of a material, the quasi-static material response is a low-frequency limit of the dynamic storage response so a strong correlation is expected [84].

The importance of our findings is that they suggest the possibility that generalized reduction in bone quality contributes to the cause of low-trauma (osteoporotic) fractures. We have demonstrated an association, and not cause-and-effect. However, the absence of an association such as we have demonstrated would make it unlikely that this new line of research would be continued in the search for causes of skeletal fragility. There are clues as to causes of reduced bone quality. While the measures of bone mass and density play important role in predicting risk of osteoporotic fractures, they only provide ~50% contribution [1, 2], and therefore, other factors including intrinsic material properties of bone tissue may also be critical. Our unique data are helpful to understand the contribution of intrinsic bone tissue material properties affecting bone quality and that they may contribute to the risk of age-related postmenopausal osteoporotic fractures [3,4] independent of bone mass and density. The lower quasi-static modulus and hardness could explain some of the osteoporotic fragility in bone tissue for the Cases. Furthermore, the bone fragility in fracturing osteoporotic women (Cases) may also come from decreased heterogeneity in both quasi-static and dynamic (viscoelastic) material properties suggesting a bone tissue (both and cortical and trabecular) with relatively uniform material properties that would contribute to lower the toughness and make the bone tissue more prone to fractures [32,37,49,55]. With everything being equal regarding bone mass and density, the lower heterogeneity in material properties may contribute to fractures in Cases. Our findings suggest that defects in the mechanical properties in bone might be generalized, and not limited to the anatomical location of fractures. We hope that our findings stimulate further research to demonstrate a cause and effect.

This study has several limitations. The iliac crest biopsies do not represent fracture sites as reported in the Cases suggesting the possibility that intrinsic property variations may not be uniform across the skeleton. In this study, correlations between two sites (biopsy and fracture sites) could not be determined. Furthermore, fracturing skeletal sites vary (Table 1) in Cases and may or may not be correlated to the intrinsic properties of bone biopsies as reported here. Although not measured here, the size and shape [85–88] of fracturing skeletal sites play a significant role in their strength or fracture. Nevertheless, the intrinsic (local) material properties of bone tissue along with shape and size may also have critical impacts on its strength and fracture. The anatomical direction/orientation of the bone tissue (both cortical and trabecular) within each biopsy was not certain. Furthermore, unlike whole bone mechanical testing [89], in which bone samples are often loaded to failure, the nanoindentation [46] testing in this study does not directly quantify the post-yield behavior of the material, and therefore, the toughness of material cannot be determined from the reported measurements. All specimens were embedded in a quick setting plastic (epoxy resin, Epothin, Buehler, IL, Methods section). While other sources of heterogeneity-related energy dissipation exists during skeletal loading (e.g. micro crack formation and propagation, de-bonding at the cement lines, etc.) [90–92], we only characterized the deformation of the bone tissue at the local level using the indenter tip. Therefore, the heterogeneity in local intrinsic strength variables of bone tissue properties may be at the nano and micro length scale only.

The cortical indents were in the interstitial bone tissue, where the “mineral/matrix” composite is older [27,34–39] and is relatively more prone to microdamage [24,93]. Interstitial bone is mostly in a steady state in adults, i.e. “older” than Haversian bone. Only about 3% of cortical (Haversian) bone turns over annually, thus, there would be mostly “old” steady state bone in the cortex, while trabecular bone turns over at a rate of about 12–13% per year [94].



The viscoelasticity makes bone tissue sensitive to nanoindentation testing conditions (both preparation methods and testing) and induces variability [95–100]. The specimens tested in a dehydrated condition have a higher modulus than that in a wet condition [99,100]. All the specimens in this study were hydrated and processed using uniform preparation, embedding, and testing techniques in order to minimize variation. Although the results should be compared with the published data that were obtained in similar conditions [95], the importance of our data is in the relative difference (modulus, hardness, heterogeneity, etc.) between the Cases and Controls.

Furthermore, the lack of a significant correlation between mineral composition [28] and the mechanical properties could be because our data came from two different biopsies (each from the same subject) which were subjected to different processing and embedding techniques (e.g. hydrated bone tissue in epoxy resin for nanomechanical vs. dehydrated tissue embedded in PMMA for FTIR technique). Finally, only the cortical bone tissue showed mechanical property differences in median values between Cases and Controls. While in agreement with other study [46] for differences in hardness and similarity in quasi-static modulus [83], properties between trabecular and cortical bone tissue, this is the first comprehensive study of comparing trabecular and cortical bone tissue. The lack of difference (Cases vs. Control) in trabecular bone could be due to the fact that the turnover rate in trabecular bone is faster [17,94,101] resulting in mineral and collagen properties different than cortical bone, where the mineral/collagen has more maturation (old mineral, greater hardness), and therefore, reflects different intrinsic properties [46] that are sensitive to fracture status in women.

Another limitation is related to the statistical analysis. Most of the nanoindentation measures have asymmetric (non-normal) distributions. Most of the analyses reported here are based on ranks of values rather than the values themselves, but particularly the logistic regression is subject to problems when variables with highly non-normal distributions are included. In addition, we saw several moderate to strong correlations among the nanoindentation measures, which can make multivariate regression results unstable. Even when comparing the two groups, the individual nanoindentation variables, there were 18 statistical tests performed, and no adjustment was made for multiple comparisons. Application of the Bonferroni adjustment to these tests showed the only significant difference to be in Variance SV-Cort-E. We believe that this application is misleadingly conservative, but we acknowledge the risk that reliance on the nominal probability values may cause us to observe significant differences between fracturing and non-fracturing subjects in variables which actually differ only by chance. For these reasons our results should be regarded as tentative.

In summary, the results of this nano indentation testing of bone tissue suggest that both median hardness and indentation modulus of the cortical bone in Controls were greater than in Cases. In addition, greater heterogeneity (variation) in hardness and modulus (for both cortical and trabecular bone) in Controls helps with energy absorption or toughness (improved bone quality) characteristics of the bone composite at the nano scale level [32,49,51]. Although, the ultrastructural details were not measured in these biopsies, the variation in both the quasi static and dynamic testing variables shows greater heterogeneity in Controls as compared to the Cases. Finally, this is the first comprehensive study to investigate the intrinsic properties of bone tissue in fracturing and non-fracturing postmenopausal women. However, because the results show surprisingly little difference in the bone properties between the Cases and Control specimens, the results may indicate that other factors (such as the spatial organization of the bone constituents) may play a much larger role than expected. Additional research into investigation of ultrastructural (nano level < 1  $\mu$ m) heterogeneity and its clinical relevance will be helpful in the testing of this hypothesis.

## Disclosures

No conflict of interest to declare.

## Acknowledgement

This project was funded by NIH (R01 AR054496-01A1, Dr. Recker, PI). Thanks to Mr. Brad Hugenroth for his input and editing.

Authors' roles: Study Design: RRR, JL, MPA, JAT. Data collection: SV, AD, JAT, MPA. Data analysis: JAT, PW. Data interpretation: RRR, JL, MPA, JAT. Drafting manuscript: All authors contributed to drafting, critically revising and approving the final version of this manuscript.

## References

- [1] M.L. Bouxsein, Mechanisms of osteoporosis therapy: A bone strength perspective, *Clin. Cornerstone* (Suppl. 2) (2003) S13–S21.
- [2] P.D. Delmas, E. Seeman, Changes in bone mineral density explain little of the reduction in vertebral or nonvertebral fracture risk with anti-resorptive therapy, *Bone* 34 (2004) 599–604.
- [3] E.S. Siris, S. Baim, A. Nattiv, Primary care use of FRAX: Absolute fracture risk assessment in postmenopausal women and older men, *Postgrad. Med.* 122 (2010) 82–90.
- [4] E.S. Siris, S.K. Brenneman, E. Barrett-Connor, P.D. Miller, S. Sajjan, M.L. Berger, Y.T. Chen, The effect of age and bone mineral density on the absolute, excess, and relative risk of fracture in postmenopausal women aged 50–99: Results from the national osteoporosis risk assessment (NORA), *Osteoporos. Int.* 17 (2006) 565–574.
- [5] R.P. Heaney, Is the paradigm shifting? *Bone* 33 (2003) 457–465.
- [6] M.J. Barger Lux, R.R. Recker, Bone microstructure in osteoporosis: Transilial biopsy and histomorphometry, *Top. Magn. Reson. Imaging* 13 (2002) 297–305.
- [7] T. Mashiba, S. Mori, D.B. Burr, S. Komatsubara, Y. Cao, T. Manabe, H. Norimatsu, The effects of suppressed bone remodeling by bisphosphonates on microdamage accumulation and degree of mineralization in the cortical bone of dog rib, *J. Bone Miner. Metab.* 23 (2005) 36–42 Suppl.
- [8] D.B. Burr, L. Miller, M. Grynpas, J. Li, A. Boyde, T. Mashiba, T. Hirano, C.C. Johnston, Tissue mineralization is increased following 1-year treatment with high doses of bisphosphonates in dogs, *Bone* 33 (2003) 960–969.
- [9] C.V. Odvina, J.E. Zerwekh, D.S. Rao, N. Maalouf, F.A. Gottschalk, C.Y. Pak, Severely suppressed bone turnover: a potential complication of alendronate therapy, *J. Clin. Endocrinol. Metab.* 90 (2005) 1294–1301.
- [10] M. Ding, J.S. Day, D.B. Burr, T. Mashiba, T. Hirano, H. Weinans, D.R. Sumner, I. Hvid, Canine cancellous bone microarchitecture after one year of high-dose bisphosphonates, *Calcif. Tissue Int.* 72 (2003) 737–744.
- [11] J.S. Day, M. Ding, P. Bednarz, J.C. van der Linden, T. Mashiba, T. Hirano, C.C. Johnston, T.A. Abbott, Predictive value of low BMD for 1-year fracture outcomes is similar for postmenopausal women ages 50–64 and 65 and older: Results from the national osteoporosis risk assessment (NORA), *J. Bone Miner. Res.* 19 (2004) 1215–1220.
- [12] S.L. Hui, C.W. Slemenda, C.C. Johnston Jr., Age and bone mass as predictors of fracture in a prospective study, *J. Clin. Invest.* 81 (1988) 1804–1809.
- [13] E.S. Siris, S.K. Brenneman, P.D. Miller, E. Barrett-Connor, Y.T. Chen, L.M. Sherwood, T.A. Abbott, Predictive value of low BMD for 1-year fracture outcomes is similar for postmenopausal women ages 50–64 and 65 and older: Results from the national osteoporosis risk assessment (NORA), *J. Bone Miner. Res.* 19 (2004) 1215–1220.
- [14] L. Mosekilde, L. Mosekilde, Iliac crest trabecular bone volume as predictor for vertebral compressive strength, ash density and trabecular bone volume in normal individuals, *Bone* 9 (1988) 195–199.
- [15] R. Recker, J. Lappe, K.M. Davies, R. Heaney, Bone remodeling increases substantially in the years after menopause and remains increased in older osteoporosis patients, *J. Bone Miner. Res.* 19 (2004) 1628–1633.
- [16] D.W. Dempster, J.E. Compston, M.K. Drezner, F.H. Glorieux, J.A. Kanis, H. Malluche, P.J. Meunier, S.M. Ott, R.R. Recker, A.M. Parfitt, Standardized nomenclature, symbols, and units for bone histomorphometry: A 2012 update of the report of the ASBMR histomorphometry nomenclature committee, *J. Bone Miner. Res.* 28 (2013) 2–17.
- [17] R.R. Recker, D.B. Kimmel, A.M. Parfitt, K.M. Davies, N. Keshawar, S. Henders, Static and tetracycline-based bone histomorphometric data from 34 normal postmenopausal females, *J. Bone Miner. Res.* 3 (1988) 133–144.
- [18] P.K. Zysset, X.E. Guo, C.E. Hoffer, K.E. Moore, S.A. Goldstein, Elastic modulus and hardness of cortical and trabecular bone lamellae measured by nanoindentation in the human femur, *J. Biomech.* 32 (1999) 1005–1012.
- [19] C.H. Turner, M. Eich, Ultrasonic velocity as a predictor of strength in bovine cancellous bone, *Calcif. Tissue Int.* 49 (1991) 116–119.
- [20] M.P. Akhter, Z. Fan, J.Y. Rho, Bone intrinsic material properties in three inbred mouse strains, *Calcif. Tissue Int.* 75 (2004) 416–420.
- [21] B. Busa, L.M. Miller, C.T. Rubin, Y.X. Qin, S. Judex, Rapid establishment of chemical and mechanical properties during lamellar bone formation, *Calcif. Tissue Int.* 77 (2005) 386–394.
- [22] N. Rodriguez-Florez, M.L. Oyen, S.J. Shefelbine, Insight into differences in nanoindentation properties of bone, *J. Mech. Behav. Biomed. Mater.* 18 (2013) 90–99.
- [23] L.P. Mullins, V. Sassi, P.E. McHugh, M.S. Bruzzi, Differences in the crack resistance of interstitial, osteonal and trabecular bone tissue, *Ann. Biomed. Eng.* 37 (2009) 2574–2582.
- [24] C.E. Hoffer, K.E. Moore, K. Kozloff, P.K. Zysset, M.B. Brown, S.A. Goldstein, Heterogeneity of bone lamellar-level elastic moduli, *Bone* 26 (2000) 603–609.
- [25] C.E. Hoffer, K.E. Moore, K. Kozloff, P.K. Zysset, S.A. Goldstein, Age, gender, and bone lamellae elastic moduli, *J. Orthop. Res.* 18 (2000) 432–437.



- [26] B.J. Polly, P.A. Yuya, M.P. Akhter, R.R. Recker, J.A. Turner, Intrinsic material properties of trabecular bone by nanoindentation testing of biopsies taken from healthy women before and after menopause, *Calcif. Tissue Int.* 26 (2011).
- [27] J.Y. Rho, P. Zioupos, J.D. Currey, G.M. Pharr, Microstructural elasticity and regional heterogeneity in human femoral bone of various ages examined by nano-indentation, *J. Biomech.* 35 (2002) 189–198.
- [28] A.L. Boskey, E. Donnelly, E. Boskey, L. Spevak, Y. Ma, W. Zhang, J. Lappe, R.R. Recker, Examining the relationships between bone tissue composition, compositional heterogeneity and fragility fracture: A matched case controlled FTIR study, *J. Bone Miner. Res.* (2015).
- [29] W.C. Oliver, G.M. Pharr, An improved technique for determining hardness and elastic modulus using load displacement sensing indentation experiments, *J. Mater. Res.* 7 (1992) 1564.
- [30] H.S. Gupta, S. Schratte, W. Tesch, P. Roschger, A. Berzlanovich, T. Schoeberl, K. Klaushofer, P. Fratzl, Two different correlations between nanoindentation modulus and mineral content in the bone-cartilage interface, *J. Struct. Biol.* 149 (2005) 138–148.
- [31] G.E. Lopez Franco, R.D. Blank, M.P. Akhter, Intrinsic material properties of cortical bone, *J. Bone Miner. Metab.* (2010).
- [32] H. Yao, M. Dao, D. Carnelli, K. Tai, C. Ortiz, Size-dependent heterogeneity benefits the mechanical performance of bone, *J. Mech. Phys. Solids* 59 (2011) 64–74.
- [33] E. Donnelly, S.P. Baker, A.L. Boskey, M.C. van der Meulen, Effects of surface roughness and maximum load on the mechanical properties of cancellous bone measured by nanoindentation, *J. Biomed. Mater. Res. A* 77 (2006) 426–435.
- [34] R.K. Nalla, J.J. Kruzic, J.H. Kinney, R.O. Ritchie, Effect of aging on the toughness of human cortical bone: evaluation by R-curves, *Bone* 35 (2004) 1240–1246.
- [35] R.K. Nalla, J.J. Kruzic, R.O. Ritchie, On the origin of the toughness of mineralized tissue: microcracking or crack bridging? *Bone* 34 (2004) 790–798.
- [36] J.G. Skedros, J.L. Holmes, E.G. Vajda, R.D. Bloebaum, Cement lines of secondary osteons in human bone are not mineral-deficient: new data in a historical perspective, *Anat. Rec. A: Discov. Mol. Cell. Evol. Biol.* 286 (2005) 781–803.
- [37] J.B. Phelps, G.B. Hubbard, X. Wang, C.M. Agrawal, Microstructural heterogeneity and the fracture toughness of bone, *J. Biomed. Mater. Res.* 51 (2000) 735–741.
- [38] T. Diab, D. Vashishth, Morphology, localization and accumulation of in vivo microdamage in human cortical bone, *Bone* 40 (2007) 612–618.
- [39] T. Diab, S. Sit, D. Kim, J. Rho, D. Vashishth, Age-dependent fatigue behavior of human cortical bone, *Eur. J. Morphol.* 42 (2005) 53–59.
- [40] S. Hengsbarger, J. Enstroem, F. Peyrin, P. Zysset, How is the indentation modulus of bone tissue related to its macroscopic elastic response? A validation study, *J. Biomech.* 36 (2003) 1503–1509.
- [41] C.K. Tjhia, C.V. Odvina, D.S. Rao, S.M. Stover, X. Wang, D.P. Fyhrie, Mechanical property and tissue mineral density differences among severely suppressed bone turnover (SSBT) patients, osteoporotic patients, and normal subjects, *Bone* 49 (2011) 1279–1289.
- [42] G. Kim, J.H. Cole, A.L. Boskey, S.P. Baker, M.C. van der Meulen, Reduced tissue-level stiffness and mineralization in osteoporotic cancellous bone, *Calcif. Tissue Int.* 95 (2014) 125–131.
- [43] M.L. Oyen, Relating viscoelastic nanoindentation creep and load relaxation experiments, *Int. J. Mater. Res.* 99 (2008) 823–828.
- [44] D.T. Reilly, A.H. Burstein, Review article, the mechanical properties of cortical bone, *J. Bone Joint Surg. Am.* 56 (1974) 1001–1022.
- [45] D.T. Reilly, A.H. Burstein, V.H. Frankel, The elastic modulus for bone, *J. Biomech.* 7 (1974) 271–275.
- [46] J.Y. Rho, T.Y. Tsui, G.M. Pharr, Elastic properties of human cortical and trabecular lamellar bone measured by nanoindentation, *Biomaterials* 18 (1997) 1325–1330.
- [47] E.S. Bessman, D.R. Carter, J.C. McCarthy, W.H. Harris, Accuracy enhancement of in vivo bone strain measurements and analysis, *J. Biomech. Eng.* 104 (1982) 226–231.
- [48] E. Donnelly, R.M. Williams, S.A. Downs, M.E. Dickinson, S.P. Baker, M.C.H. van der Meulen, Quasistatic and dynamic nanomechanical properties of cancellous bone tissue relate to collagen content and organization, *J. Mater. Res.* 21 (2006) 2106–2117.
- [49] K. Tai, M. Dao, S. Suresh, A. Palazoglu, C. Ortiz, Nanoscale heterogeneity promotes energy dissipation in bone, *Nat. Mater.* 6 (2007) 454–462.
- [50] K. Tai, F.J. Ulm, C. Ortiz, Nanogranular origins of the strength of bone, *Nano Lett.* 6 (2006) 2520–2525.
- [51] K. Tai, H.J. Qi, C. Ortiz, Effect of mineral content on the nanoindentation properties and nanoscale deformation mechanisms of bovine tibial cortical bone, *J. Mater. Sci. Mater. Med.* 16 (2005) 947–959.
- [52] S. Suresh, Graded materials for resistance to contact deformation and damage, *Science* 292 (2001) 2447–2451.
- [53] H. Gupta, P. Fratzl, M. Kerschnitzki, S. Krauss, J. Seto, W. Wagermaier, G. Benecke, P. Boesack, S. Funari, J. Currey, J. Estevez, Mechanisms of bone deformation and fracture, *Bone* 46 (2010) 512.
- [54] H.S. Gupta, J. Seto, W. Wagermaier, P. Zaslansky, P. Boesack, P. Fratzl, Cooperative deformation of mineral and collagen in bone at the nanoscale, *Proc. Natl. Acad. Sci. U. S. A.* 103 (2006) 17741–17746.
- [55] M.B. Schaffler, K. Choi, C. Milgrom, Aging and matrix microdamage accumulation in human compact bone, *Bone* 17 (1995) 521–525.
- [56] L.P. Mullins, M.S. Bruzzi, P.E. McHugh, Measurement of the microstructural fracture toughness of cortical bone using indentation fracture, *J. Biomech.* 40 (2007) 3285–3288.
- [57] E.A. Zimmermann, R.O. Ritchie, Bone as a structural material, *Adv. Healthc. Mater.* 4 (2015) 1287–1304.
- [58] N. Cuadrado, J. Seuba, D. Casellas, M. Anglada, E. Jimenez-Pique, Geometry of nano-indentation cube-corner cracks observed by FIB tomography: implication for fracture resistance estimation, *J. Eur. Ceram. Soc.* 35 (2015) 2949–2955.
- [59] R.O. Ritchie, The conflicts between strength and toughness, *Nat. Mater.* 10 (2011) 817–822.
- [60] M.D. Demetriou, M.E. Launey, G. Garrett, J.P. Schramm, D.C. Hofmann, W.L. Johnson, R.O. Ritchie, A damage-tolerant glass, *Nat. Mater.* 10 (2011) 123–128.
- [61] A. Carriero, E.A. Zimmermann, S.J. Shefelbine, R.O. Ritchie, A methodology for the investigation of toughness and crack propagation in mouse bone, *J. Mech. Behav. Biomed. Mater.* 39 (2014) 38–47.
- [62] X. Wang, D. Sudhaker Rao, L. Ajdelsztajn, T.E. Ciarelli, E.J. Laverna, D.P. Fyhrie, Human iliac crest cancellous bone elastic modulus and hardness differ with bone formation rate per bone surface but not by existence of prevalent vertebral fracture, *J. Biomed. Mater. Res. B Appl. Biomater.* 85 (2008) 68–77.
- [63] E. Donnelly, D.S. Meredith, J.T. Nguyen, A.L. Boskey, Bone tissue composition varies across anatomic sites in the proximal femur and the iliac crest, *J. Orthop. Res.* 30 (2012) 700–706.
- [64] P.D. Ross, Y.F. He, J.W. Davis, R.S. Epstein, R.D. Wasnich, Normal ranges for bone loss rates, *J. Bone Miner.* 26 (1994) 169–180.
- [65] N. Fratzl-Zelman, P. Roschger, A. Gourrier, M. Weber, B.M. Misof, N. Loveridge, J. Reeve, K. Klaushofer, P. Fratzl, Combination of nanoindentation and quantitative backscattered electron imaging revealed altered bone material properties associated with femoral neck fragility, *Calcif. Tissue Int.* 85 (2009) 335–343.
- [66] G. Kim, A.L. Boskey, S.P. Baker, M.C. van der Meulen, Improved prediction of rat cortical bone mechanical behavior using composite beam theory to integrate tissue level properties, *J. Biomech.* 45 (2012) 2784–2790.
- [67] L.M. Miller, W. Little, A. Schirmer, F. Sheikh, B. Busa, S. Judex, Accretion of bone quantity and quality in the developing mouse skeleton, *J. Bone Miner. Res.* 22 (2007) 1037–1045.
- [68] E. Donnelly, A.L. Boskey, S.P. Baker, M.C. van der Meulen, Effects of tissue age on bone tissue material composition and nanomechanical properties in the rat cortex, *J. Biomed. Mater. Res. A* 92 (2010) 1048–1056.
- [69] J. Burket, S. Gourrier-Arsiquaud, L.M. Havill, S.P. Baker, A.L. Boskey, M.C. van der Meulen, Microstructure and nanomechanical properties in osteons relate to tissue and animal age, *J. Biomech.* 44 (2011) 277–284.
- [70] J.C. Burket, D.J. Brooks, J.M. MacLeay, S.P. Baker, A.L. Boskey, M.C. van der Meulen, Variations in nanomechanical properties and tissue composition within trabeculae from an ovine model of osteoporosis and treatment, *Bone* 52 (2013) 326–336.
- [71] H.H. Malluche, D.S. Porter, M.C. Monier-Faugere, H. Mawad, D. Pienkowski, Differences in bone quality in low- and high-turnover renal osteodystrophy, *J. Am. Soc. Nephrol.* 23 (2012) 525–532.
- [72] P. Fratzl, Bone fracture: When the cracks begin to show, *Nat. Mater.* 7 (2008) 610–612.
- [73] P. Fratzl, H.S. Gupta, F.D. Fischer, O. Kolednik, Hindered crack propagation in materials with periodically varying young's modulus - lessons from biological materials, *Adv. Mater.* 19 (2007) 2657 (+).
- [74] H. Peterlik, P. Roschger, K. Klaushofer, P. Fratzl, From brittle to ductile fracture of bone, *Nat. Mater.* 5 (2006) 52–55.
- [75] B. Busse, M. Hahn, M. Soltan, J. Zustin, K. Puschel, G.N. Duda, M. Amling, Increased calcium content and inhomogeneity of mineralization render bone toughness in osteoporosis: mineralization, morphology and biomechanics of human single trabeculae, *Bone* 45 (2009) 1034–1043.
- [76] L.J. van Ruijven, L. Mulder, T.M. van Eijden, Variations in mineralization affect the stress and strain distributions in cortical and trabecular bone, *J. Biomech.* 40 (2007) 1211–1218.
- [77] J. Rho, L. Kuhn-Spearing, P. Zioupos, Mechanical properties and the hierarchical structure of bone, *Med. Eng. Phys.* (1998).
- [78] R.O. Ritchie, M.J. Buehler, P. Hansma, Plasticity and toughness in bone, *Phys. Today* 62 (2009) 41–47.
- [79] H. Gupta, W. Wagermaier, G. Zickler, D. Aroush, S. Funari, P. Roschger, H. Wagner, P. Fratzl, Nanoscale deformation mechanisms in bone, *Nano Lett.* 5 (2005) 2108–2111.
- [80] S. Pathak, J.G. Swadener, S.R. Kalidindi, H. Courtland, K.J. Jepsen, H.M. Goldman, Measuring the dynamic mechanical response of hydrated mouse bone by nanoindentation, *J. Mech. Behav. Biomed. Mater.* 4 (2011) 34–43.
- [81] C.H. Turner, J. Rho, Y. Takano, T.Y. Tsui, G.M. Pharr, The elastic properties of trabecular and cortical bone tissues are similar: results from two microscopic measurement techniques, *J. Biomech.* 32 (1999) 437–441.
- [82] Z. Fan, P.A. Smith, E.C. Eckstein, G.F. Harris, Mechanical properties of OI type III bone tissue measured by nanoindentation, *J. Biomed. Mater. Res. A* 79 (2006) 71–77.
- [83] Z. Fan, P.A. Smith, G.F. Harris, F. Rauch, R. Bajorunaite, Comparison of nanoindentation measurements between osteogenesis imperfecta type III and type IV and between different anatomic locations (femur/tibia versus iliac crest), *Connect. Tissue Res.* 48 (2007) 70–75.
- [84] S.N. Raja, S. Basu, A.M. Limaye, T.J. Anderson, C.M. Hyland, L. Lin, A.P. Alivisatos, R.O. Ritchie, Strain-dependent dynamic mechanical properties of keylar to failure: structural correlations and comparisons to other polymers, *Mater. Today* 2 (2015) E33–E37 Communications.
- [85] J.D. Currey, Mechanical properties of bone tissues with greatly differing functions, *J. Biomech.* 12 (1979) 313–319.
- [86] P. Zioupos, A. Casinos, Cumulative damage and the response of human bone in two-step loading fatigue, *J. Biomech.* 31 (1998) 825–833.
- [87] C.H. Turner, Bone strength: Current concepts, *Ann. N. Y. Acad. Sci.* (2006) (Hormones).
- [88] C.H. Turner, Biomechanics of bone: determinants of skeletal fragility and bone quality, *Osteoporos. Int.* (2002).
- [89] J.D. Currey, K. Brear, P. Zioupos, The effects of ageing and changes in mineral content in degrading the toughness of human femora, *J. Biomech.* 29 (1996) 257–260.

- [90] L.J. Bonderer, A.R. Studart, L.J. FAU-Gauckler, L.J. Gauckler, Bioinspired design and assembly of platelet reinforced polymer films, *Science* 319 (5866) (2008 Feb 22) 1069–1073, <http://dx.doi.org/10.1126/science.1148726>.
- [91] H.S. Gupta, U. Stachewicz, W. Wagermaier, P. Roschger, H.D. Wagner, P. Fratzl, Mechanical modulation at the lamellar level in osteonal bone, *J. Mater. Res.* 21 (2006) 1913–1921.
- [92] P. Fratzl, R. Weinkamer, Nature's hierarchical materials, *Prog. Mater. Sci.* 52 (2007) 1263–1334.
- [93] J.S. Yerramshetty, O. Akkus, The associations between mineral crystallinity and the mechanical properties of human cortical bone, *Bone* 42 (2008) 476–482.
- [94] R.R. Recker, *Bone Biopsy and Histomorphometry in Clinical Practice: Primer on the Metabolic Bone Diseases and Disorders of Mineral Metabolism*, Eighth Edition ed. John Wiley & Sons, Inc, USA, 2013 307.
- [95] G. Lewis, J.S. Nyman, The use of nanoindentation for characterizing the properties of mineralized hard tissues: state-of-the art review, *J. Biomed. Mater. Res. B Appl. Biomater.* 87 (2008) 286–301.
- [96] J.Y. Rho, G.M. Pharr, Effects of drying on the mechanical properties of bovine femur measured by nanoindentation, *J. Mater. Sci. Mater. Med.* 10 (1999) 485–488.
- [97] C. Albert, J. Jameson, J.M. Toth, P. Smith, G. Harris, Bone properties by nanoindentation in mild and severe osteogenesis imperfecta, *Clin. Biomech. (Bristol, Avon)* 28 (2013) 110–116.
- [98] E. Mittra, C. Rubin, Y.X. Qin, Interrelationship of trabecular mechanical and microstructural properties in sheep trabecular bone, *J. Biomech.* 38 (2005) 1229–1237.
- [99] C.E. Hoffler, X.E. Guo, P.K. Zysset, S.A. Goldstein, An application of nanoindentation technique to measure bone tissue lamellae properties, *J. Biomech. Eng.* 127 (2005) 1046–1053.
- [100] A.J. Bushby, V.L. Ferguson, A. Boyde, Nanoindentation of bone: Comparison of specimens tested in liquid and embedded in polymethylmethacrylate (vol 19, pg 249, 2004), *J. Mater. Res.* 19 (2004) 1581.
- [101] A.M. Parfitt, C.H. Mathews, A.R. Villanueva, M. Kleerekoper, B. Frame, D.S. Rao, Relationships between surface, volume, and thickness of iliac trabecular bone in aging and in osteoporosis. Implications for the microanatomic and cellular mechanisms of bone loss, *J. Clin. Invest.* 72 (1983) 1396–1409.
- [102] M.F. Doerner, W.D. Nix, An improved technique for determining the data from depth-sensing indentation instruments, *J. Mater. Res.* (1986).